Supporting Information

Three-Dimensional Perovskite Nanophotonic Wire Array-Based Light-Emitting Diodes with Significantly Improved Efficiency and Stability

Qianpeng Zhang,[1] Daquan Zhang,[1,2] Leilei Gu,[1,2] Kwong-Hoi Tsui,[1] Swapnadeep Poddar,[1] Yu Fu,[1,2] Lei Shu,[1] and Zhiyong Fan[1,2,*]

[1]Department of Electronic & Computer Engineering, The Hong Kong University of Science and Technology, Clear Water Bay, Hong Kong

[2]HKUST-Shenzhen Research Institute, No. 9 Yuexing first RD, South Area, Hi-tech Park, Nanshan, Shenzhen 518057, China

[*]Corresponding to eezfan@ust.hk

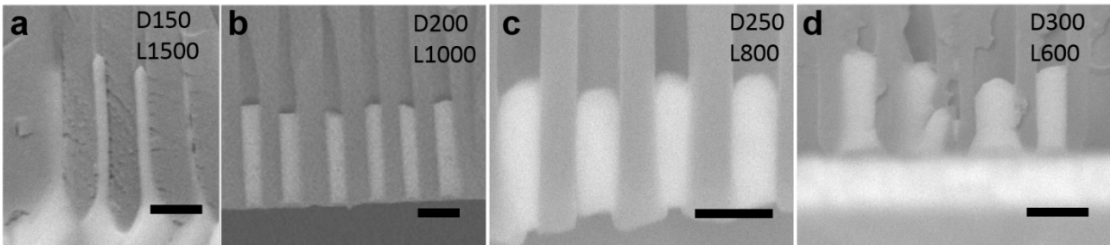

Figure S1. Cross-sectional SEM images showing PNWs with (a) 140 nm diameter and 1500 nm length; (b) 200 nm diameter and 1000 nm length; (c) 240 nm diameter and 800 nm length; (d) 300 nm diameter and 300 nm length. All scale bars are 500 nm.

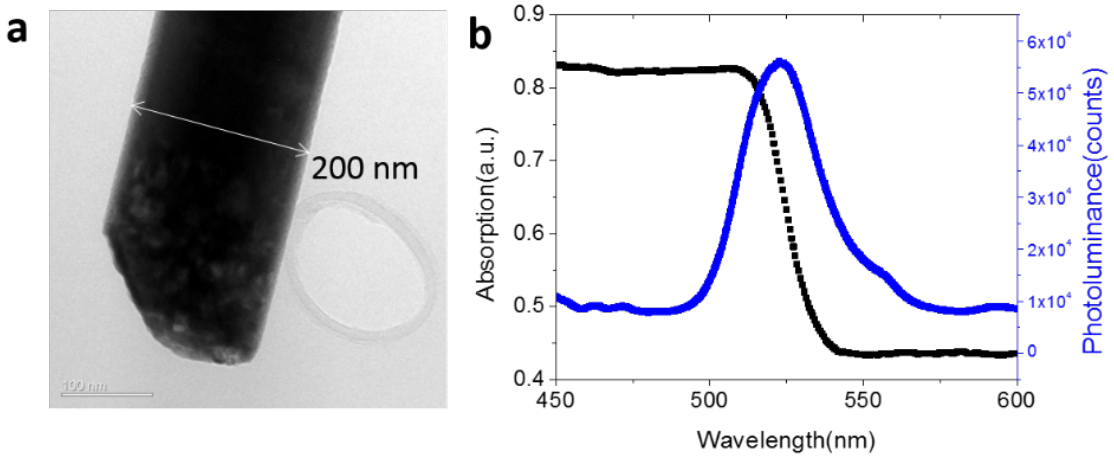

Figure S2. (a) Transmission electron microscopy (TEM) image of a PNW with 200 nm diameter. (b) Absorption and photoluminescence spectra of the PNWs.

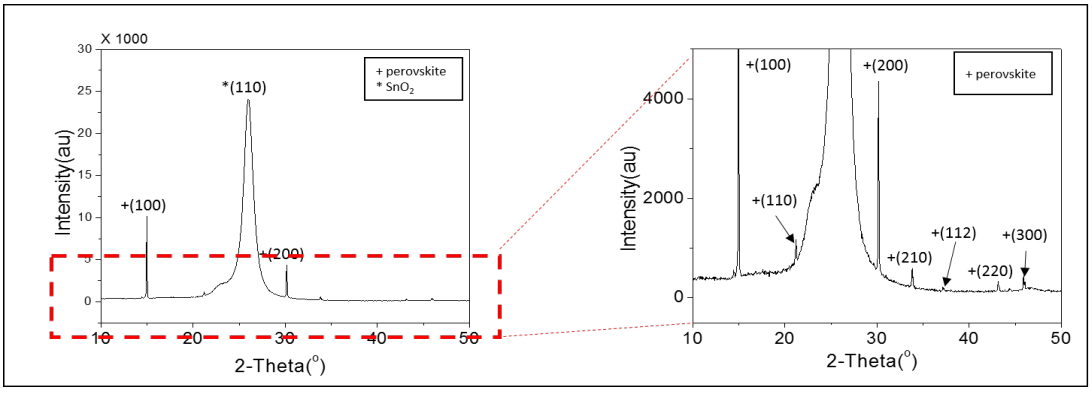

Figure S3. X-ray diffraction (XRD) of PNWs on ITO glass.

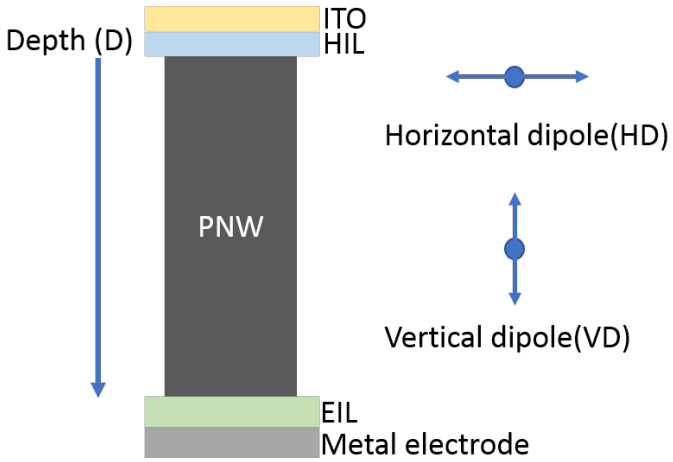

Figure S4. Diagram showing the dipole position and directions in the PNW. Depth is the distance from the interface of HIL/PNW.

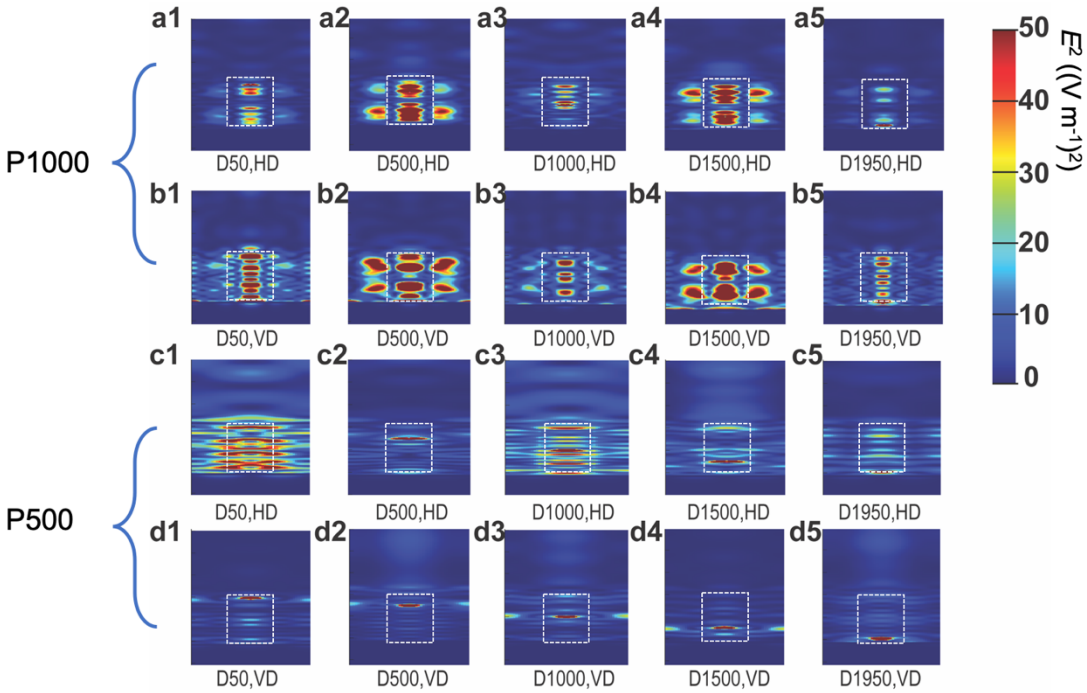

Figure S5. Cross-sectional E^2 $(Vm^{-1})^2$ at emission wavelength 530 nm for **a1-a5** and **b1-b5** 1000 nm pitch (P1000) and 400 nm diameter PNWs. **c1-c5** and **d1-d5** for 500 nm pitch (P500) and 200 nm diameter PNWs. Different dipole positions are used. D50, D500, D1000, D1500, and D1950 mean the dipole is 50 nm, 500 nm, 1000 nm, 1500 nm and 1950 nm from the top surface, respectively. HD and VD mean the dipole polarizations are

horizontal and vertical directions, respectively. White dash lines showing the PNW position. Light is propagating upwards. All the figures have the same color bar range to make a fair comparison on E^2 field patterns of both inside and outside the PNWs among different cases.

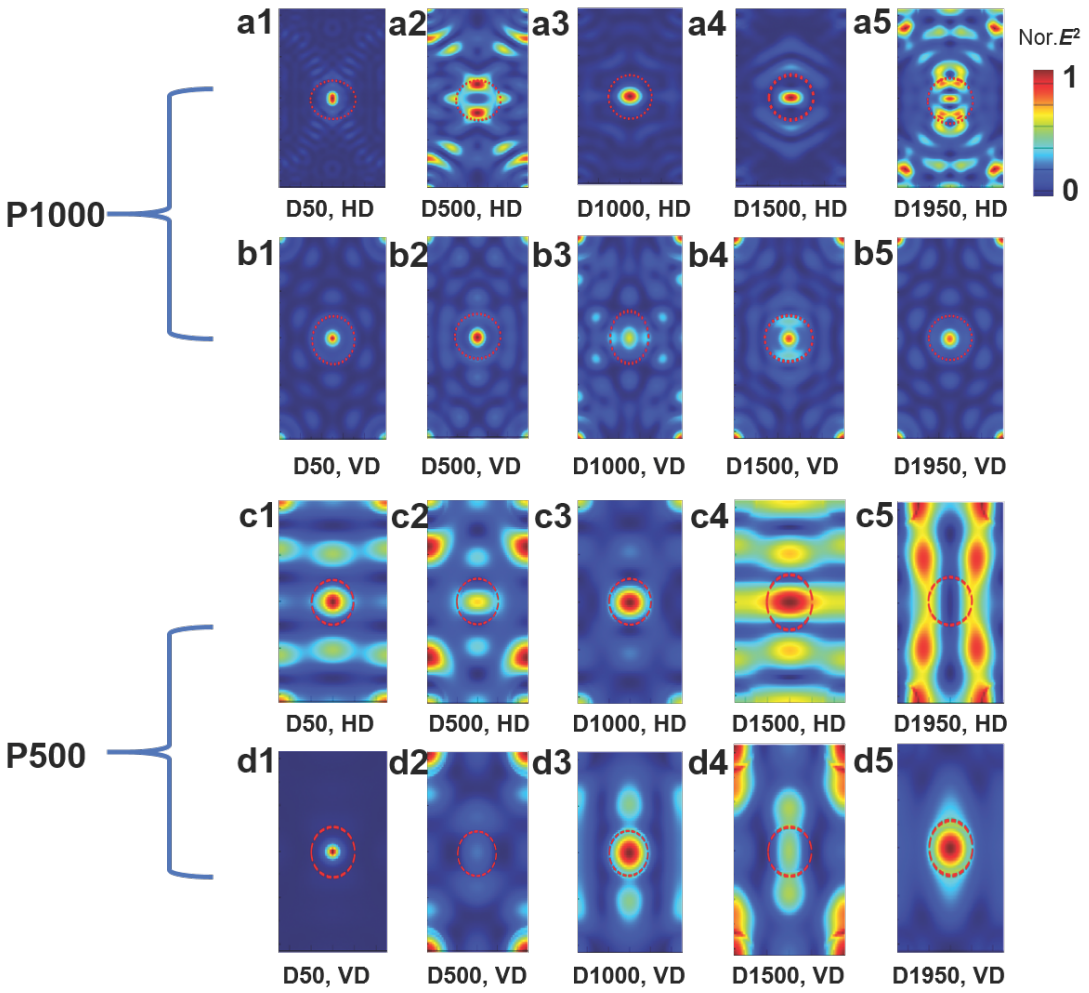

Figure S6. Normalized E^2 patterns (at emission wavelength 530 nm) at the PNW emitter top surface. All color scales are fitted to the best view for each individual case. **a1**-**a5** and **b1**-**b5** for 1000 nm pitch (P1000) and 400 nm diameter PNWs, **c1**-**c5** and **d1**-**d5** for 500 nm pitch (P500) and 200 nm diameter PNWs. Different dipole positions are used. D50, D500, D1000, D1500, and D1950 means the dipole is 50 nm, 500 nm, 1000 nm, 1500 nm and 1950 nm from the top surface, respectively. HD and VD mean the dipole polarizations are horizontal and vertical directions, respectively.

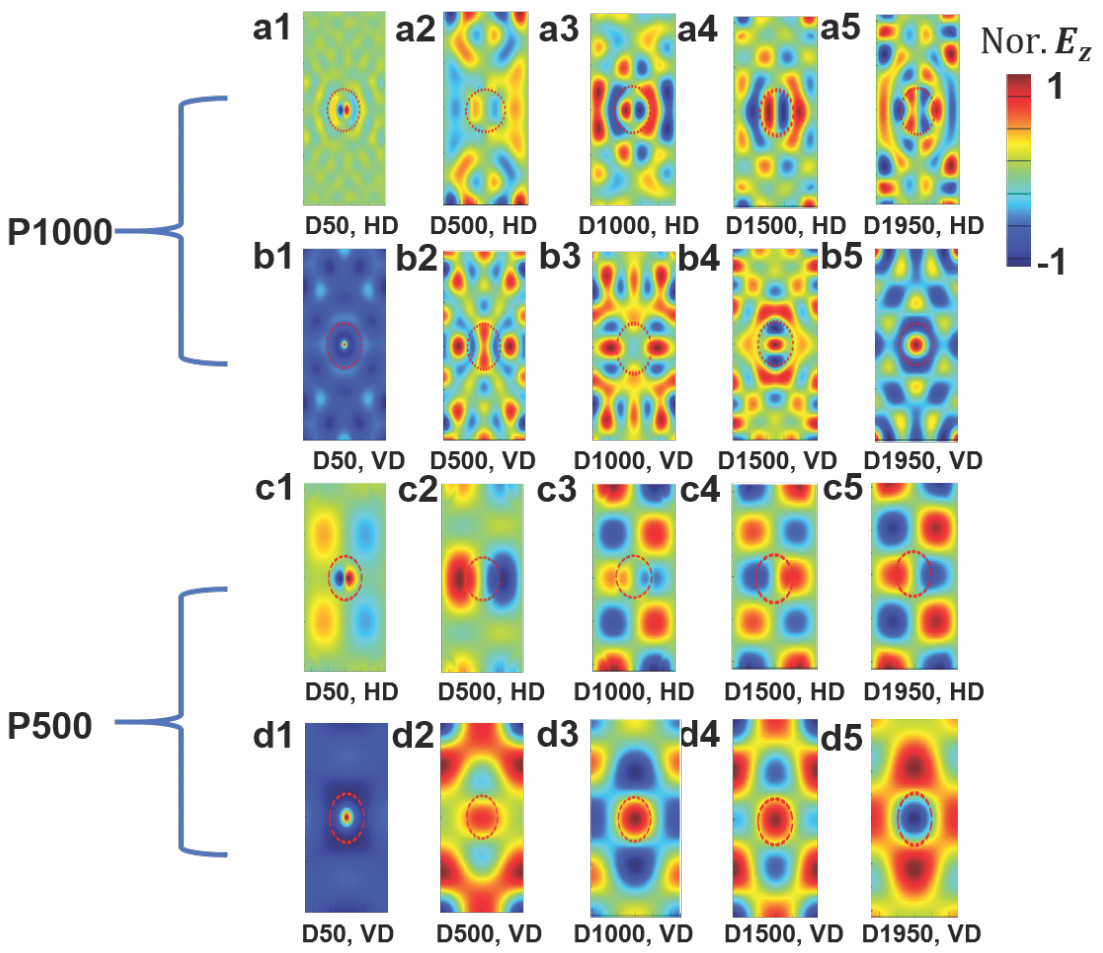

Figure S7. Normalized E_z patterns at the PNW emitter top surface (at 530 nm). All color scales are fitted to the best view for each individual case. **a1**-**a5** and **b1**-**b5** for P1000D400 PNWs, **c1**-**c5** and **d1**-**d5** for P500D200 PNWs. Different dipole positions are used. D50, D500, D1000, D1500, and D1950 mean the dipole is 50 nm, 500 nm, 1000 nm, 1500 nm and 1950 nm from the top surface, respectively. HD and VD mean the dipole polarizations are horizontal and vertical directions, respectively.

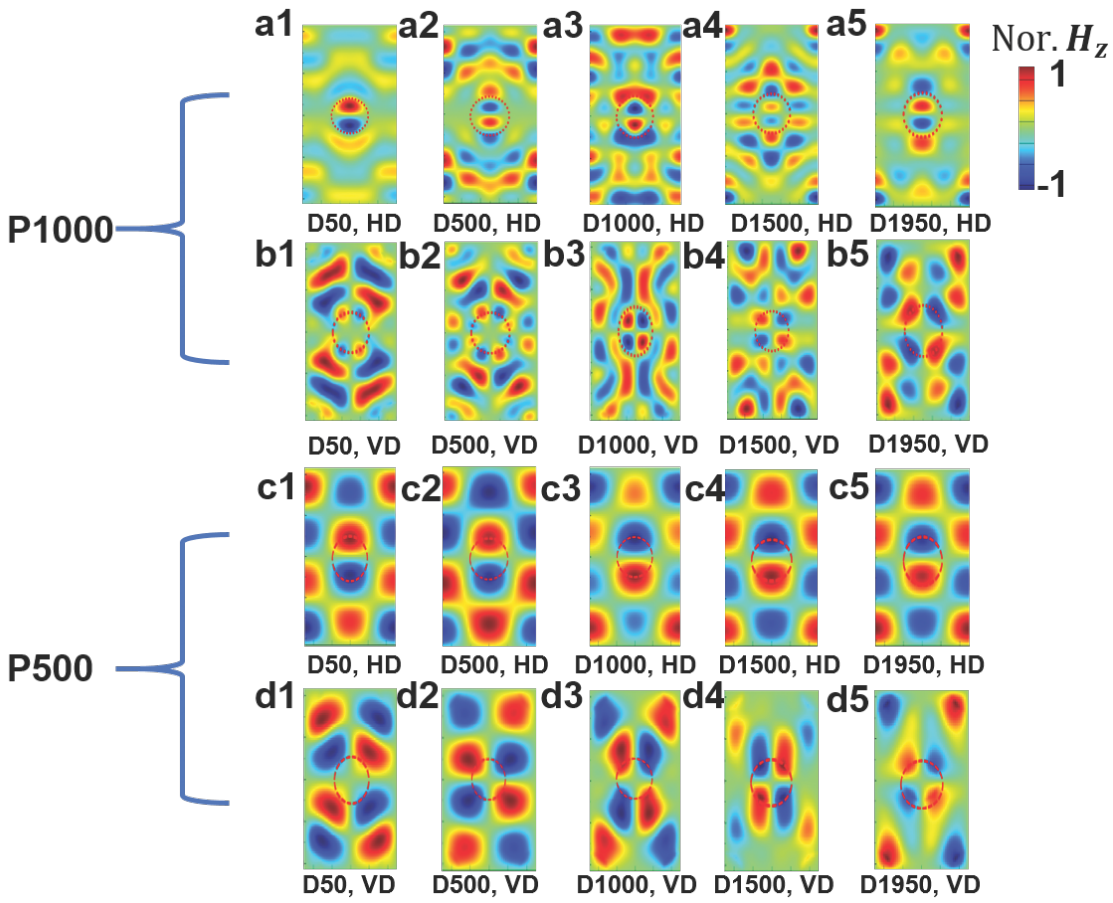

Figure S8. Normalized H_z patterns at the PNW emitter top surface (at 530 nm). All color scales are fitted to the best view for each individual case. **a1**-**a5** and **b1**-**b5** for P1000D400 PNWs, **c1**-**c5** and **d1**-**d5** for P500D200 PNWs. Different dipole positions are used. D50, D500, D1000, D1500, and D1950 mean the dipole is 50 nm, 500 nm, 1000 nm, 1500 nm and 1950 nm from the top surface, respectively. HD and VD mean the dipole polarizations are horizontal and vertical directions, respectively.

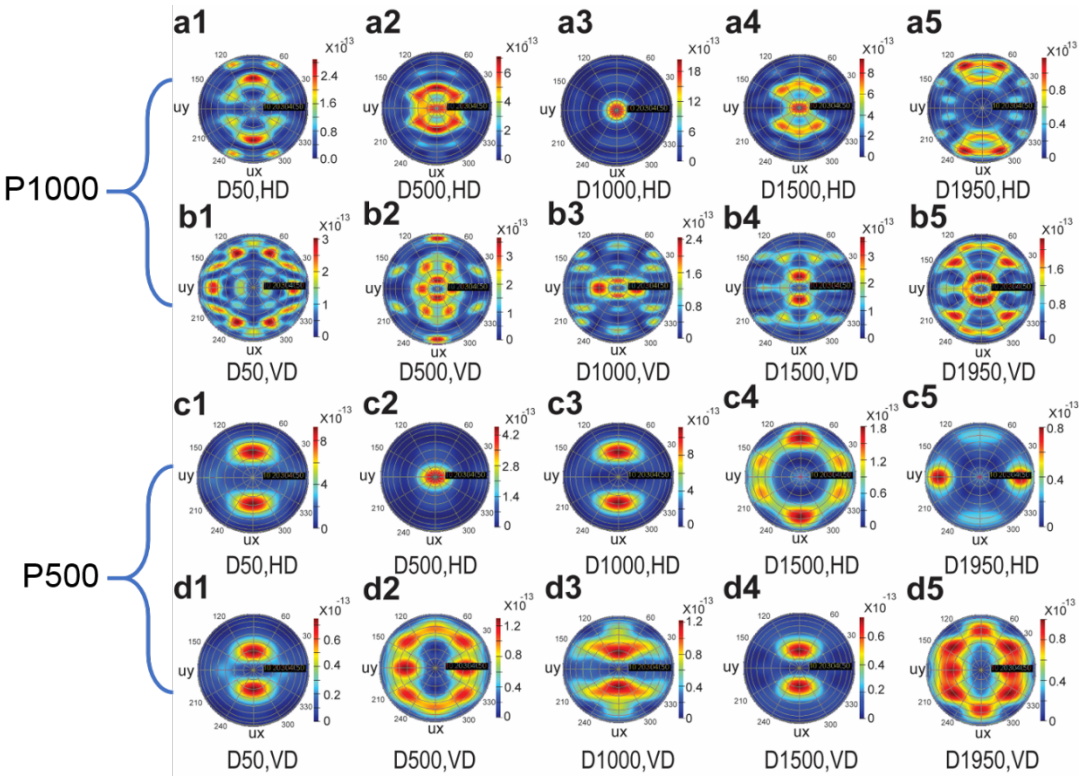

Figure S9. Far-field E^2 $(Vm^{-1})^2$ **a1-a5** and **b1-b5** for 1000 nm pitch and 400 nm diameter PNWs, **c1-c5** and **d1-d5** for 500 nm pitch and 200 nm diameter PNWs. Different dipole positions are used. D50, D500, D1000, D1500, and D1950 mean the dipole is 50 nm, 500 nm, 1000 nm, 1500 nm and 1950 nm from the top surface, respectively. HD and VD mean the dipole polarizations are horizontal and vertical directions, respectively.

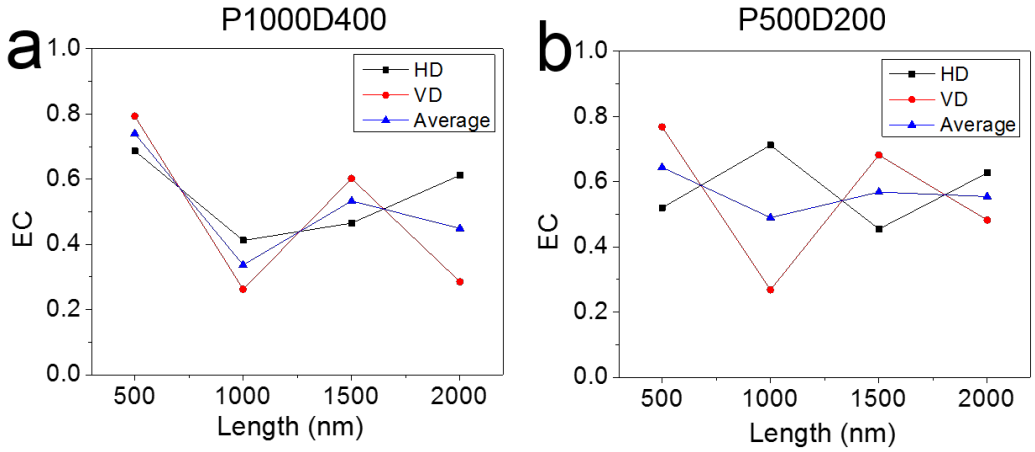

Figure S10. Length effect for PNWs with different lengths. (a) P1000D400 PNWs, (b) P500D200 PNWs.

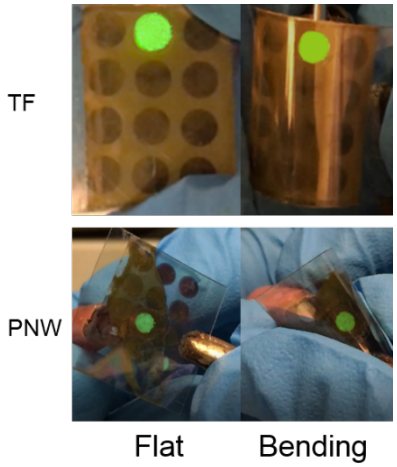

Figure S11. Optical photo of thin-film (TF) and perovskite nanophotonic wire (PNW) devices at flat and bending situations.

Table S1. Extraction coefficients (EC) of the pitch 500 nm diameter 200 nm PNWs with different dipole positions. Half *r* here indicates that the dipole is half radius away from the PNW axis.

	EC		EC
p500-d200-hd-depth 100nm	0.419	p500-d200-hd-depth 100nm-half r	0.460
p500-d200-vd-depth 100nm	0.691	p500-d200-vd-depth 100nm-half r	0.515
p500-d200-hd-depth 200nm	0.440	p500-d200-hd-depth 200nm-half r	0.565
p500-d200-vd-depth 200nm	0.661	p500-d200-vd-depth 200nm-half r	0.571
p500-d200-hd-depth 300nm	0.413	p500-d200-hd-depth 300nm-half r	0.624
p500-d200-vd-depth 300nm	0.655	p500-d200-vd-depth 300nm-half r	0.633
p500-d200-hd-depth 400nm	0.461	p500-d200-hd-depth 400nm-half r	0.585
p500-d200-vd-depth 400nm	0.416	p500-d200-vd-depth 400nm-half r	0.438
p500-d200-hd-depth 500nm	0.540	p500-d200-hd-depth 500nm-half r	0.582
p500-d200-vd-depth 500nm	0.606	p500-d200-vd-depth 500nm-half r	0.594
p500-d200-hd-depth 600nm	0.447	p500-d200-hd-depth 600nm-half r	0.675
p500-d200-vd-depth 600nm	0.214	p500-d200-vd-depth 600nm-half r	0.285
p500-d200-hd-depth 700nm	0.463	p500-d200-hd-depth 700nm-half r	0.357
p500-d200-vd-depth 700nm	0.615	p500-d200-vd-depth 700nm-half r	0.432
p500-d200-hd-depth 800nm	0.499	p500-d200-hd-depth 800nm-half r	0.401
p500-d200-vd-depth 800nm	0.353	p500-d200-vd-depth 800nm-half r	0.390
p500-d200-hd-depth 900nm	0.435	p500-d200-hd-depth 900nm-half r	0.571
p500-d200-vd-depth 900nm	0.608	p500-d200-vd-depth 900nm-half r	0.397
p500-d200-hd-depth 1000nm	0.627	p500-d200-hd-depth 1000nm-half r	0.573
p500-d200-vd-depth 1000nm	0.482	p500-d200-vd-depth 1000nm-half r	0.379
p500-d200-hd-depth 1100nm	0.491	p500-d200-hd-depth 1100nm-half r	0.378
p500-d200-vd-depth 1100nm	0.385	p500-d200-vd-depth 1100nm-half r	0.389
p500-d200-hd-depth 1200nm	0.476	p500-d200-hd-depth 1200nm-half r	0.621
p500-d200-vd-depth 1200nm	0.631	p500-d200-vd-depth 1200nm-half r	0.523
p500-d200-hd-depth 1300nm	0.912	p500-d200-hd-depth 1300nm-half r	0.541
p500-d200-vd-depth 1300nm	0.161	p500-d200-vd-depth 1300nm-half r	0.287
p500-d200-hd-depth 1400nm	0.399	p500-d200-hd-depth 1400nm-half r	0.474
p500-d200-vd-depth 1400nm	0.655	p500-d200-vd-depth 1400nm-half r	0.636
p500-d200-hd-depth 1500nm	0.630	p500-d200-hd-depth 1500nm-half r	0.655
p500-d200-vd-depth 1500nm	0.300	p500-d200-vd-depth 1500nm-half r	0.377
p500-d200-hd-depth 1600nm	0.730	p500-d200-hd-depth 1600nm-half r	0.637
p500-d200-vd-depth 1600nm	0.684	p500-d200-vd-depth 1600nm-half r	0.456
p500-d200-hd-depth 1700nm	0.432	p500-d200-hd-depth 1700nm-half r	0.458
p500-d200-vd-depth 1700nm	0.596	p500-d200-vd-depth 1700nm-half r	0.626
p500-d200-hd-depth 1800nm	0.439	p500-d200-hd-depth 1800nm-half r	0.649
p500-d200-vd-depth 1800nm	0.784	p500-d200-vd-depth 1800nm-half r	0.536
p500-d200-hd-depth 1900nm	0.530	p500-d200-hd-depth 1900nm-half r	0.595
p500-d200-vd-depth 1900nm	0.753	p500-d200-vd-depth 1900nm-half r	0.317

average	0.527		0.505

Table S2. Comparison of the T50s of the reported high-efficiency perovskite LEDs and our perovskite PNW LEDs.[1-10]

	T50	Material
Z. Wei, et. al., Nanoscale, 2016	Stable L > 100 cd m^{-2} for >15 h in ambient air @ 66.67 mA cm^{-2}	$CsPbBr_3$+CsBr
L. Zhang, et. al., Nat. Comm., 2016	~13-15 mins, @5V bias, max ~ 250 cdm^{-2}	$Cs_{0.87}MA_{0.13}PbBr_3$ with PVP
N. Wang, et. al., Nat. Photonics, 2016	~100 mins @10 mA cm^{-2}	$NFPI_7$ MQWs (Infrared)
Z. Xiao, et. al., Nat. Photonics, 2016	>90s without degradation @5V; storage >100 days without degradation	$MAPbBr_3$+BABr
W. Zou, et. al., Nat. Comm., 2018	30 mins, @100 mA cm^{-2}, glass-epoxy encapsulation	MQWs (Infrared)
K. Lin, et. al., Nature, 2018	~10 mins, @167mA cm^{-2}, max 7,130 cd m^{-2}; 104.56h @ 100 cdm^{-2}	$CsPbBr_3$ +MABr
Y. Cao, et. al., Nature 2018	20 h @100 $mAcm^{-2}$, glass-epoxy encapsulation	$FAPbI_3$ +5AVA (Infrared)
T. Chiba, et. al., Nat. Photonics, 2018	5 mins @1.25 $mAcm^{-2}$, OAM-I-based QDs; 180 min @1.25 mA cm^{-2}, An-HI-based QDs	$CsPbBr_3$ QDs with anion exchange (Red)
B. Zhao, et. al., Nat. Photonics, 2018	46 h @ 0.1 $mAcm^{-2}$,	NMAI: FAI: PbI_2: poly-HEMA=5:3:8:4, perovskite-polymer bulk heterostructure (PPBH) (Infrared)
W. Xu, et. al., Nat. Photonics, 2019	20 h @25 $mAcm^{-2}$,	ODEA treated $FAPbI_3$ (Infrared)
Our work	37 mins @4V, 20$mAcm^{-2}$, max ~10, 000 cd^{-2}.	MABr:$CsPbBr_3$ NWs

Reference

1. Wei, Z.; Perumal, A.; Su, R.; Sushant, S.; Xing, J.; Zhang, Q.; Tan, S. T.; Demir, H. V.; Xiong, Q., Solution-Processed Highly Bright and Durable Cesium Lead Halide Perovskite Light-Emitting Diodes. *Nanoscale* **2016,** *8*, 18021-18026.
2. Zhang, L.; Yang, X.; Jiang, Q.; Wang, P.; Yin, Z.; Zhang, X.; Tan, H.; Yang, Y. M.; Wei, M.; Sutherland, B. R., Ultra-Bright and Highly Efficient Inorganic Based Perovskite Light-Emitting Diodes. *Nat. Commun.* **2017,** *8*, 15640.
3. Wang, N.; Cheng, L.; Ge, R.; Zhang, S.; Miao, Y.; Zou, W.; Yi, C.; Sun, Y.; Cao, Y.; Yang, R., Perovskite Light-Emitting Diodes Based on Solution-Processed Self-Organized Multiple Quantum Wells. *Nat. Photonics* **2016,** *10*, 699-704.
4. Xiao, Z.; Kerner, R. A.; Zhao, L.; Tran, N. L.; Lee, K. M.; Koh, T.-W.; Scholes, G. D.; Rand, B. P., Efficient Perovskite Light-Emitting Diodes Featuring Nanometre-Sized Crystallites. *Nat. Photonics* **2017,** *11*, 108-115.
5. Zou, W.; Li, R.; Zhang, S.; Liu, Y.; Wang, N.; Cao, Y.; Miao, Y.; Xu, M.; Guo, Q.; Di, D., Minimising Efficiency Roll-Off in High-Brightness Perovskite Light-Emitting Diodes. *Nat. Commun.* **2018,** *9*, 608.
6. Lin, K.; Xing, J.; Quan, L. N.; de Arquer, F. P. G.; Gong, X.; Lu, J.; Xie, L.; Zhao, W.; Zhang, D.; Yan, C.; Li, W.; Liu, X.; Lu, Y.; Kirman, J.; Sargent, E. H.; Xiong, Q.;

Wei, Z., Perovskite Light-Emitting Diodes with External Quantum Efficiency Exceeding 20 Per Cent. *Nature* **2018,** *562*, 245-248.
7. Cao, Y.; Wang, N.; Tian, H.; Guo, J.; Wei, Y.; Chen, H.; Miao, Y.; Zou, W.; Pan, K.; He, Y.; Cao, H.; Ke, Y.; Xu, M.; Wang, Y.; Yang, M.; Du, K.; Fu, Z.; Kong, D.; Dai, D.; Jin, Y.; Li, G.; Li, H.; Peng, Q.; Wang, J.; Huang, W., Perovskite Light-Emitting Diodes Based on Spontaneously Formed Submicrometre-Scale Structures. *Nature* **2018,** *562*, 249-253.
8. Chiba, T.; Hayashi, Y.; Ebe, H.; Hoshi, K.; Sato, J.; Sato, S.; Pu, Y.-J.; Ohisa, S.; Kido, J., Anion-Exchange Red Perovskite Quantum Dots with Ammonium Iodine Salts for Highly Efficient Light-Emitting Devices. *Nat. Photonics* **2018,** *12*, 681-687.
9. Zhao, B.; Bai, S.; Kim, V.; Lamboll, R.; Shivanna, R.; Auras, F.; Richter, J. M.; Yang, L.; Dai, L.; Alsari, M., High-Efficiency Perovskite–Polymer Bulk Heterostructure Light-Emitting Diodes. *Nat. Photonics* **2018,** *12*, 783-789.
10. Xu, W.; Hu, Q.; Bai, S.; Bao, C.; Miao, Y.; Yuan, Z.; Borzda, T.; Barker, A. J.; Tyukalova, E.; Hu, Z., Rational Molecular Passivation for High-Performance Perovskite Light-Emitting Diodes. *Nat. Photonics* **2019,** *13*, 418-424.